

Article

Thermodynamic and Transport Properties of Biomass-Derived Furfural, Furfuryl Alcohol and Their Mixtures

Zoran V. Simić¹, Mirjana Lj. Kijevčanin², Ivona R. Radović², Miha Grilc³  and Gorica R. Ivaniš^{2,3,*}

¹ Innovation Center of the Faculty of Technology and Metallurgy, University of Belgrade, 11120 Belgrade, Serbia; zsimic@tmf.bg.ac.rs

² Faculty of Technology and Metallurgy, University of Belgrade, 11120 Belgrade, Serbia; mirjana@tmf.bg.ac.rs (M.L.K.); ivonag@tmf.bg.ac.rs (I.R.R.)

³ Department of Catalysis and Chemical Reaction Engineering, National Institute of Chemistry, 1000 Ljubljana, Slovenia; miha.grilc@ki.si

* Correspondence: gorica.ivanis@ki.si; Tel.: +386-1-4760540

Abstract: The limited reserves and well-known disadvantages of using fossil energy sources have increased the need for appropriate renewable substitutes in the production of various chemicals and materials. Biomass has been shown to be worthy of attention since it can be converted to biofuels and value-added chemicals relatively easily. The design of biomass valorisation process requires knowledge on the thermodynamic behaviour of the biomass-derived compounds, such as furfural and furfuryl alcohol. The thermodynamic and transport properties of the binary system furfural + furfuryl alcohol were studied at various temperatures and pressures. Density, speed of sound and refractive index were measured in the temperature range $T = (288.15\text{--}345.15)$ K and viscosity was measured at temperatures up to 373.15 K, all at atmospheric pressure. Further, the density of pure components was obtained in the temperature range (293.15–413.15) K for furfural and (293.15–373.15) K for furfuryl alcohol at pressures up to 60.0 MPa. The obtained density values were correlated using the modified Tammann–Tait equation with an average absolute deviation lower than 0.009% for furfural and furfuryl alcohol. The optimised parameters were used for the calculation of the isothermal compressibility, the isobaric thermal expansivity, the internal pressure and the isobaric and isochoric specific heat capacities. The reported data are a valuable source of information for the further application of the investigated compounds.

Keywords: density; speed of sound; viscosity; refractive index; modelling; binary mixtures; high pressure



Citation: Simić, Z.V.; Kijevčanin, M.L.; Radović, I.R.; Grilc, M.; Ivaniš, G.R. Thermodynamic and Transport Properties of Biomass-Derived Furfural, Furfuryl Alcohol and Their Mixtures. *Energies* **2021**, *14*, 7769. <https://doi.org/10.3390/en14227769>

Academic Editor: William E. Acree, Jr.

Received: 18 October 2021

Accepted: 15 November 2021

Published: 19 November 2021

Publisher's Note: MDPI stays neutral with regard to jurisdictional claims in published maps and institutional affiliations.



Copyright: © 2021 by the authors. Licensee MDPI, Basel, Switzerland. This article is an open access article distributed under the terms and conditions of the Creative Commons Attribution (CC BY) license (<https://creativecommons.org/licenses/by/4.0/>).

1. Introduction

Due to increasing environmental pollution caused by the use of fossil fuels and the depletion of their reserves, there is an increasing need for renewable energy sources that would meet the basic principles of “green” chemistry, as defined by Anastas and Warner [1]. The transition from today’s economy based on fossil fuels to a sustainable bio-based economy is a great challenge. Biomass has appeared as a promising, carbon-neutral substitute for fossil fuels in terms of energy production and the production of various chemicals and materials. In particular, lignocellulosic biomass has gained significant attention due to its low cost, less waste and being the most abundant biopolymer in nature [2]. It mainly consists of three components, i.e., cellulose and hemicellulose that compose of polysaccharides, and lignin, an aromatic polymer [3]. Lignocellulose has shown a great potential in production of platform chemicals that can be further converted to added-value chemicals by a hydrodeoxygenation process (HDO). The design of biomass valorisation processes, as well as the collection and handling the obtained products, requires the knowledge on thermodynamic behaviour of all components present in the process in order to maximise efficiency and avoid unnecessary energy consumption. Furthermore,

HDO consists of complex reactions that overlap and entail accurate microkinetic models involving transfer phenomena and thermodynamic properties of the compounds [4].

Some promising compounds produced from biomass are furfural and furfuryl alcohol. Furfural is one of the furan derivatives formed from the hemicellulose part of lignocellulose and is a very important platform chemical that can be transformed to widely used chemicals and fuels [5]. Nowadays, its production is based on hydrothermal conversion of biomass, particularly, pentosan sugars are hydrolysed to monosaccharides which are further transferred to furfural by dehydration [5–8]. The efficiency of the conversion depends strongly on reaction condition, used catalyst and solvent, and the optimisation of these three parameters is subject of many research [7,9]. Furfuryl alcohol is often used in the production of resins, pharmaceuticals and fragrances, and it is typically produced by the selective hydrogenation of furfural [5,10]. The world annual production of furfural has been estimated to over 300 ktons and about 65% of that is used in the production of furfuryl alcohol [5].

Despite the great range of the application of furfural and furfuryl alcohol, such as solvents, biofuels, an alternative to the production of antacids, fertilizers, plastics and paints [11], the thermodynamic properties of furfural, furfuryl alcohol, and especially their mixtures are not enough studied. Lomba et al. [12] performed thorough study of physicochemical properties of biomass-derived green solvents. They modelled density, refractive index, speed of sound, surface tension, dynamic viscosity, static permittivity and vapour pressure of furfural and furfuryl alcohol at temperatures (279.15–338.15) K and seemingly at atmospheric pressure. Bendiaf et al. [13] studied density and speed of sound of furfural mixtures with different alcohols, and Zaoui-Djelloul-Daouadji et al. [14] reported the same properties for furfuryl alcohol and its mixtures with toluene or ethanol, at temperatures (283.15–313.15) K and 0.1 MPa. Almeida et al. [15] presented density and refractive index data of furfural at (288.15–318.15) K and atmospheric pressure (≈ 95 kPa), whereas Hough et al. [16] reported density of furfuryl alcohol at temperatures (303.15–343.15) K within a study of the heat capacities of organic liquids at atmospheric pressure. Further, Qureshi et al. [17] presented data on density and viscosity of furfuryl alcohol in the temperature range (288.15–318.15) K at 0.1 MPa within their study on biofuel-relevant compounds. Nduli and Deenadayalu [18] reported density, speed of sound and refractive index of furfural and furfuryl alcohol at temperatures (298.15–318.15) K, while Mahi et al. [19] gave the same thermodynamic properties but only for furfuryl alcohol in the temperature interval (293.15–323.15) K, all at atmospheric pressure. More recently, Belhadj et al. [20] published the density, speed of sound and refractive index of furfural at temperatures (293.15–323.15) K and pressure of 0.1 MPa.

In addition to the thermodynamic properties at atmospheric pressure, it is necessary to know the thermodynamic behaviour at high pressures and temperatures, because many processes as well as HDO [21] take place under such conditions. Only two papers reporting thermodynamic properties of furfural or furfuryl alcohol at higher temperatures and pressures were found during a literature review. Guerrero et al. [22] studied density and the derived thermodynamic properties of furfural and furfuryl alcohol at pressures up to 60 MPa, and at temperatures (283.15–338.15) K. In the second mentioned paper, Baird et al. [23] studied vapour pressures and densities of various bio-compounds and reported density of furfural in the wide range of temperature (293.15–448.15) K at pressures up to about 10 MPa. To the best of our knowledge, there are no published data on density, viscosity, speed of sound and refractive index of binary mixtures furfural + furfuryl alcohol.

In this paper, density, speed of sound and refractive index of furfural, furfuryl alcohol and their binary mixtures are reported at temperature range (288.15–343.15) K and 0.1 MPa while their viscosities are obtained under the same pressure over the temperature range (288.15–373.15) K. Further, the densities of the pure components are measured at higher pressures, up to 60 MPa, and in the temperature interval (293.15–413.15) K for furfural and (293.15–373.15) K for furfuryl alcohol. The high-pressure density data were fitted to the modified Tammann–Tait equation [24], which enabled the determination of the derived

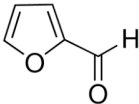
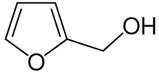
thermodynamic properties, such as the isothermal compressibility, κ_T , isobaric thermal expansivity, α_p , the internal pressure, p_{int} , and the difference in isobaric and isochoric heat capacities, $c_p - c_v$. In addition, isobaric and isochoric specific heat capacities for furfural and furfuryl alcohol at 0.1 MPa were calculated.

2. Experimental Section

2.1. Chemicals

Furfural (99 wt.%) was supplied by Sigma-Aldrich (St. Louis, MO 63103, USA) and furfuryl alcohol (98 wt.%) was purchased from Aldrich Chemicals (St. Louis, MO 63103, USA) (Table 1). Both chemicals were degassed prior to measurements.

Table 1. The chemicals used in the measurements.

Chemical Name	CAS Reg. No.	Structure	Supplier	Purity, Mass Fraction
Furfural	98-01-1		Sigma-Aldrich	0.99
Furfuryl alcohol	98-00-0		Aldrich Chemicals	0.98

2.2. Apparatus and Procedure

All experimental data in this paper were obtained using high precision instrumentation from the manufacturer Anton Paar (8054 Graz, Austria). Density, ρ , at atmospheric pressure and speed of sound, u , were determined by means of DSA 5000 M. The DSA 5000 M device (Anton Paar, 8054 Graz, Austria) enables the measurement of density in the range of (0–3) $\text{g}\cdot\text{cm}^{-3}$ and speed of sound within the interval (1000–2000) $\text{m}\cdot\text{s}^{-1}$, both at temperatures (273.15–343.15) K. The device contains two measuring cells: one made of stainless steel used for measuring of speed of sound passing through the sample and U-shaped tube made of borosilicate glass where density is measured. Densities are calculated from the oscillation period of U tube filled with sample with automatic viscosity correction. The calibration of the device is performed daily using ambient air and ultra-pure water.

Dynamic viscosity, η , at atmospheric pressure was measured using Stabinger viscometer SVM 3000/G2 (Anton Paar, 8054 Graz, Austria). Besides dynamic viscosity in the range (0.2–20,000) $\text{mPa}\cdot\text{s}$; this device also measures kinematic viscosity in the range (0.2–20,000) $\text{mm}^2\cdot\text{s}^{-1}$ and density within (0.65–3) $\text{g}\cdot\text{cm}^{-3}$, at temperatures starting from 20 K below room temperature to 378.15 K. The SVM 3000/G2 is a rotational viscometer with a very small measuring cell containing a tube filled with sample that rotates at a constant speed and a measuring rotor, which floats in the sample. The viscosity measurement is based on the measurement of torque and speed of the rotor immersed in the sample. In addition to the cylinder for measuring the dynamic viscosity, the device also has an oscillating U-tube for density measurement.

Refractometer RXA-156 (Anton Paar, 8054 Graz, Austria) was used for the measurements of refractive index, n_D , at atmospheric pressure. The refractive index range that can be measured on this device is 1.32–1.56 at temperatures (283.15–343.15) K. The work of this refractometer is based on the measurement of the critical angle of the total reflection of light (wavelength of 589.3 nm) after passing through a sample.

The devices and the measurements procedures were described in more detail in our previous publications [25,26]. The expanded uncertainties of the performed measurements at 0.1 MPa were estimated based on the repeatability of the measurements, including the influence of samples' purities [27]. The impurities in the used chemicals were not analysed but, based on the literature [5], it was assumed that for furfural (1%) they mostly are 2-methylfuran and 2-acetyl furan and for furfuryl alcohol (2%), the expected impurities

are furfural, 2-methylfuran and resins. The density was determined with an expanded uncertainty, U , of $0.8 \text{ kg}\cdot\text{m}^{-3}$ with a 95 % level of confidence (coverage factor, $k = 2$) and the expanded uncertainties (confidence level 95 %, $k = 2$) in speed of sound, viscosity and refractive index were estimated to $0.2 \text{ m}\cdot\text{s}^{-1}$, $0.007 \text{ mPa}\cdot\text{s}$ and $2.8\cdot 10^{-3}$, respectively.

All mixtures were prepared using a Mettler Toledo AG 204 mass balance (8606 Greifensee, Switzerland) with the precision $1\cdot 10^{-7} \text{ kg}$. The estimated standard uncertainty, u , in mole fraction, x , was less than $\pm 1\cdot 10^{-4}$.

Density at higher pressures, p , up to 60 MPa and temperatures, T , in the range (293.15–413.15) K for furfural and (293.15–373.15) K for furfuryl alcohol, were experimentally determined on Anton Paar digital vibrating tube densimeter DMA HP (Anton Paar, 8054 Graz, Austria) by measuring the oscillation period of a U-shaped tube filled with the sample. The temperature of the measuring cell was precisely controlled by an integrated Peltier thermostat and the expanded uncertainty in temperature, $U(T)$ with confidence level of 95% ($k = 2$) was estimated to 0.02 K. A Pressure Generator model 50-6-15 (High Pressure Equipment Co, Erie, PA 16505, USA) was used to achieve and control the desired pressure by means of acetone as the hydraulic fluid. A Wika S-10 pressure transducer (Alexander Wiegand GmbH & Co, 63911 Klingenberg, Germany) was used for pressure detection and an estimated expanded uncertainty in pressure, 95% confidence level ($k = 2$) was 0.1 MPa. The classic calibration procedure with one reference fluid, proposed by Comuñas et al. [28], was applied to obtain density values from the measured periods of oscillations of the U-tube. A detailed description of the apparatus, vibrating tube densimeter calibration and high-pressure density measurement procedure is described elsewhere [29]. Since the measuring cell DMA HP does not provide automatic correction of density due to effect of sample's viscosity, it had to be estimated after experiment based on the information received from the supplier Anton Paar. For the studied compounds, furfural and furfuryl alcohol, the mentioned correction of the density was less than $0.08 \text{ kg}\cdot\text{m}^{-3}$. The overall combined expanded uncertainty of the reported densities measured at DMA HP measuring cell was estimated taking into account the uncertainties of all properties that affect the density measurements, such as the oscillation period of U tube, temperature and pressure, and the densities of the reference fluids. Besides that, the damping effects on the vibrating tube and the impurities present in the used chemicals were considered, which resulted in the expanded uncertainty in density, $U(\rho)$ of $0.9 \text{ kg}\cdot\text{m}^{-3}$ at temperature (293.15–363.15) K and $1.3 \text{ kg}\cdot\text{m}^{-3}$ at higher temperatures (373.15–413.15) K (confidence level 95%, $k = 2$).

3. Result and Discussion

3.1. Experimental Results

Thermodynamic properties such as density, speed of sound and refractive index of binary mixtures furfural + furfuryl alcohol, were measured at 0.1 MPa over the temperature range $T = (293.15\text{--}343.15) \text{ K}$. The dynamic viscosity of the mentioned mixtures was studied at somewhat wider temperature range of (288.15–373.15) K and the same pressure, 0.1 MPa. The results of the measurements are listed in Table 2.

In the case of furfural, the measured densities differ slightly from the values reported by Almeida et al. [15], Lomba et al. [12] and Bendiaf et al. [13], average absolute deviation (AAD) was about 0.02%, 0.03% and 0.08% ($0.3 \text{ kg}\cdot\text{m}^{-3}$, $0.4 \text{ kg}\cdot\text{m}^{-3}$ and $0.9 \text{ kg}\cdot\text{m}^{-3}$), respectively. A somewhat better agreement was observed between the measured furfural density and the data of Qureshi et al. [17] and Belhadj et al. [20] with $\text{AAD} \approx 0.02\%$ ($0.2 \text{ kg}\cdot\text{m}^{-3}$), and in the case of Nduli and Deenadayalu [18] AAD was about 0.05% ($0.6 \text{ kg}\cdot\text{m}^{-3}$). Furfural viscosities given here deviate from the data reported by Lomba et al. [12] with $\text{AAD} \approx 5.25\%$ ($0.07 \text{ mPa}\cdot\text{s}$) and from the data reported by Qureshi et al. [17] with $\text{AAD} \approx 4.67\%$ ($0.07 \text{ mPa}\cdot\text{s}$). Speed of sound measurements for furfural were in good accordance with the literature data; the deviation from the data of Bendiaf et al. [13], Lomba et al. [12] and Belhadj et al. [20] was $\text{AAD} \approx 0.02\%$ ($0.3 \text{ m}\cdot\text{s}^{-1}$), and for the data of Nduli and Deenadayalu [18] AAD was slightly higher, 0.03% ($0.4 \text{ m}\cdot\text{s}^{-1}$). Almeida et al. [15] and Lomba et al. [12] also reported refractive indices of furfural that deviate from the data

presented here with AAD of 0.07% (0.001) and 0.11% (0.002), respectively. The comparison of the measured values with the refractive index reported by Nduli and Deenadayalu [18] and Belhadj et al. [20] resulted in AAD of 0.08% (0.001) and 0.12% (0.002), respectively.

Table 2. Density, ρ , dynamic viscosity, η , speed of sound, u , and refractive index, n_D , of the binary system furfural (1) + furfuryl alcohol (2) as a function of furfural mole fraction, x_1 , at $p = 0.1$ MPa ^a.

Furfural (1) + Furfuryl Alcohol (2)						
$\rho^b/\text{kg}\cdot\text{m}^{-3}$						
T^c/K						
x_1^d	288.15	293.15	298.15	303.15	308.15	313.15
0.0000	1138.8	1134.2	1129.6	1124.9	1120.3	1115.6
0.2000	1145.3	1140.6	1135.8	1131.0	1126.2	1121.4
0.4000	1151.0	1146.1	1141.2	1136.2	1131.3	1126.4
0.6000	1156.8	1151.8	1146.7	1141.7	1136.6	1131.6
0.8001	1161.3	1156.1	1150.9	1145.8	1140.6	1135.4
1.0000	1165.5	1160.2	1154.9	1149.6	1144.2	1138.9
	318.15	323.15	328.15	333.15	338.15	343.15
0.0000	1110.8	1106.1	1101.3	1096.5	1091.7	1086.8
0.2000	1116.5	1111.6	1106.7	1101.8	1096.9	1091.9
0.4000	1121.4	1116.5	1111.6	1106.6	1101.7	1096.8
0.6000	1126.6	1121.5	1116.5	1111.5	1106.4	1101.4
0.8001	1130.3	1125.2	1120.1	1114.9	1109.8	1104.6
1.0000	1133.5	1128.1	1122.7	1117.3	1111.9	1106.4
$\eta^e/\text{mPa}\cdot\text{s}$						
T/K						
x_1	288.15	293.15	298.15	303.15	308.15	313.15
0.0000	7.056	5.886	4.934	4.216	3.635	3.160
0.2000	5.096	4.358	3.717	3.230	2.828	2.506
0.4000	3.702	3.292	2.856	2.524	2.251	2.022
0.6000	2.893	2.584	2.276	2.040	1.845	1.677
0.8001	2.244	2.042	1.827	1.665	1.538	1.414
1.0000	1.877	1.728	1.567	1.436	1.327	1.231
	318.15	323.15	328.15	333.15	338.15	343.15
0.0000	2.771	2.448	2.176	1.947	1.753	1.586
0.2000	2.227	1.994	1.795	1.626	1.480	1.353
0.4000	1.820	1.651	1.505	1.378	1.267	1.168
0.6000	1.529	1.402	1.291	1.193	1.107	1.030
0.8001	1.303	1.207	1.122	1.046	0.978	0.916
1.0000	1.145	1.068	1.000	0.938	0.883	0.832
	348.15	353.15	358.15	363.15	368.15	373.15
0.0000	1.442	1.317	1.208	1.112	1.027	0.955
0.2000	1.242	1.145	1.059	0.982	0.914	0.856
0.4000	1.082	1.005	0.936	0.874	0.818	0.770
0.6000	0.961	0.899	0.843	0.792	0.746	0.705
0.8001	0.861	0.810	0.764	0.722	0.683	0.649
1.0000	0.786	0.744	0.706	0.671	0.638	0.610

Table 2. Cont.

Furfural (1) + Furfuryl Alcohol (2)						
$u^f / \text{m}\cdot\text{s}^{-1}$						
T/K						
x_1	288.15	293.15	298.15	303.15	308.15	313.15
0.0000	1483.3	1466.9	1450.5	1434.3	1418.2	1402.1
0.2000	1487.9	1471.1	1454.3	1437.7	1421.1	1404.7
0.4000	1487.8	1470.7	1453.6	1436.7	1419.8	1403.0
0.6000	1485.9	1468.5	1451.1	1433.8	1416.5	1399.4
0.8001	1482.2	1464.3	1446.5	1428.7	1411.0	1393.4
1.0000	1477.1	1458.8	1440.5	1422.3	1404.2	1386.1
	318.15	323.15	328.15	333.15	338.15	343.15
0.0000	1386.2	1370.3	1354.5	1338.7	1322.9	1307.2
0.2000	1388.3	1372.0	1355.7	1339.4	1323.2	1307.1
0.4000	1386.2	1369.5	1352.9	1336.4	1319.8	1303.4
0.6000	1382.3	1365.3	1348.3	1331.4	1314.6	1297.8
0.8001	1375.9	1358.4	1341.1	1323.8	1306.6	1289.5
1.0000	1368.2	1350.3	1332.5	1314.7	1297.1	1279.5
n_D^g						
T/K						
x_1	288.15	293.15	298.15	303.15	308.15	313.15
0.0000	1.490	1.487	1.485	1.483	1.480	1.478
0.2000	1.498	1.496	1.494	1.491	1.489	1.487
0.4000	1.506	1.504	1.502	1.499	1.496	1.494
0.6000	1.514	1.512	1.509	1.506	1.504	1.502
0.8001	1.522	1.519	1.516	1.513	1.511	1.508
1.0000	1.528	1.525	1.522	1.519	1.517	1.514
	318.15	323.15	328.15	333.15	338.15	343.15
0.0000	1.476	1.474	1.471	1.469	1.466	1.464
0.2000	1.484	1.482	1.480	1.478	1.475	1.473
0.4000	1.492	1.489	1.487	1.484	1.482	1.479
0.6000	1.499	1.497	1.494	1.492	1.489	1.486
0.8001	1.505	1.503	1.500	1.498	1.495	1.492
1.0000	1.511	1.508	1.506	1.503	1.500	1.498

Expanded uncertainties (95% confidence level, $k = 2$): ^a $U(p) = 0.005 \text{ MPa}$; ^b $U(\rho) = 0.8 \text{ kg}\cdot\text{m}^{-3}$; ^c $U(T) = 0.02 \text{ K}$; ^d $U(x_1) = 0.0002$; ^e $U(\eta) = 0.007 \cdot \text{mPa}\cdot\text{s}$; ^f $U(u) = 0.2 \text{ m}\cdot\text{s}^{-1}$; ^g $U(n_D) = 2.8 \cdot 10^{-3}$.

The results of the measurements are compared to the data found in literature for pure furfural and furfuryl alcohol [12–20] and good agreements were noted (Figure 1).

As for furfuryl alcohol, the measured density data differ from those obtained by Hough et al. [16], Lomba et al. [12] and Zaoui-Djelloul-Daouadji et al. [14] with AAD of 0.11%, 0.06% and 0.17% ($1.2 \text{ kg}\cdot\text{m}^{-3}$, $0.7 \text{ kg}\cdot\text{m}^{-3}$ and $1.9 \text{ kg}\cdot\text{m}^{-3}$), respectively. The deviation between the measured data and the densities reported by Mahi et al. [19] was about 0.11% ($1.3 \text{ kg}\cdot\text{m}^{-3}$), but it was significantly higher for the results of Nduli and Deenadayalu [18], AAD $\approx 0.24\%$ ($2.7 \text{ kg}\cdot\text{m}^{-3}$). In the case of the viscosity of furfuryl alcohol, AAD between the data given here and those of Lomba et al. [12] was about 1.11% ($0.05 \text{ mPa}\cdot\text{s}$). The measured speed of sound of furfuryl alcohol deviates from data of Lomba et al. [12] and Zaoui-Djelloul-Daouadji et al. [14] with AAD of 0.03% and 0.16% ($0.4 \text{ m}\cdot\text{s}^{-1}$ and $2.3 \text{ m}\cdot\text{s}^{-1}$), respectively. The comparison of speed of sound data with the values reported by Mahi et al. [19] gave similar results, AAD $\approx 0.11\%$ ($0.6 \text{ m}\cdot\text{s}^{-1}$) but for the results of Nduli and Deenadayalu [18] AAD was about 0.44% ($6.2 \text{ m}\cdot\text{s}^{-1}$). Finally, Lomba et al. [12], Nduli and Deenadayalu [18] and Mahi et al. [19] also reported the refractive indices of furfuryl alcohol, which agree well with the experimental

values presented here; the AAD was about 0.09%, 0.02% and 0.04% (0.001, 0.0003 and 0.0006), respectively.

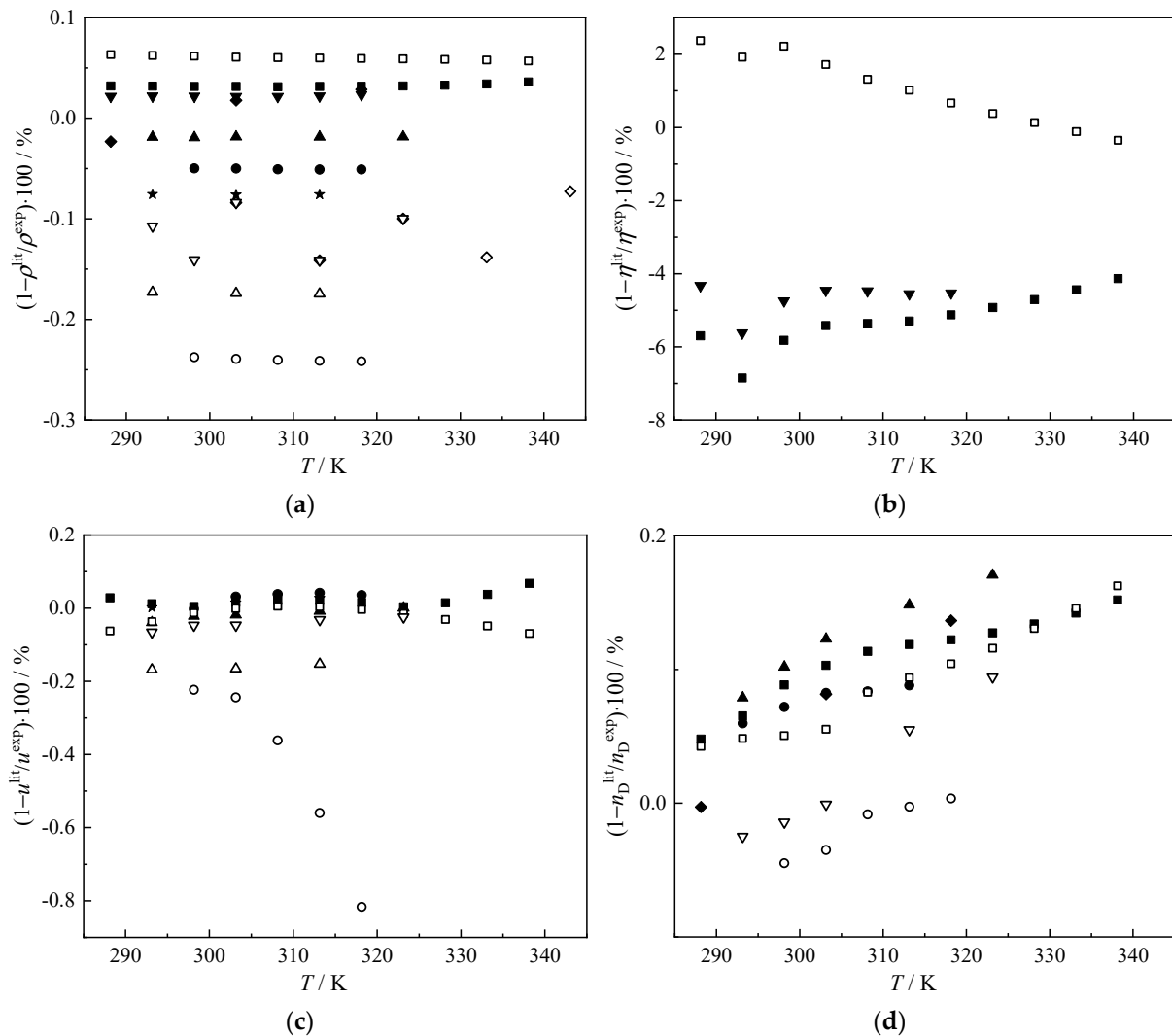


Figure 1. The percentage deviations of the measured (a) density, ρ , (b) dynamic viscosity, η , (c) speed of sound, u , and (d) refractive index, n_D , from the literature data reported by: (\blacklozenge) Almeida et al. [15], (\blackstar) Bendiaf et al. [13], (\blacksquare , \square) Lomba et al. [12], (\blacktriangle) Belhadj et al. [20], (\bullet , \circ) Nduli and Deenadayalu [18], (\blacktriangledown) Qureshi et al. [17], (\diamond) Hough et al. [16], (\triangle) Zaoui-Djelloul-Daouadji et al. [14], and (∇) Mahi et al. [19] for furfural (full symbols) and furfuryl alcohol (empty symbols).

The measurement uncertainties reported by Zaoui-Djelloul-Daouadji et al. [14], Qureshi et al. [17] and Baird et al. [23] are of the same order of magnitude as the uncertainties estimated for the results given in this work. Mahi et al. [19] and Belhadj et al. [20] assessed higher uncertainties while the uncertainties of the other compared data [12,13,15,16,18,22] were lower than those reported here. The agreement of the results presented in this paper with the literature data [12–20] is very good and falls mostly within the reported uncertainties. The unsatisfactory results were obtained only when the density and speed of sound of furfuryl alcohol were compared with the data of Zaoui-Djelloul-Daouadji et al. [14] and Nduli and Deenadayalu [18]. The comparison of experimental results with literature data performed by the mentioned authors in their papers [14,18] gave deviations similar to those obtained comparing the data presented here with their results [14,18]. Therefore, the poor agreement of the measured density and speed of sound of furfuryl alcohol with the data published in two mentioned papers [14,18] should not cast doubt on the reliability of the presented results.

Density, speed of sound and refractive index decrease linearly as a function of temperature (Figure 2). Density and refractive index increase for increasing concentration of furfural in the mixture because these thermodynamic properties of pure furfural are higher than of furfuryl alcohol. The dependence of the mentioned properties on the furfural fraction in the mixtures is given at Figure S1. The density, speed of sound and refractive index measured for the studied mixtures are higher than the values that would be expected for ideal mixture (based on Kay's rule). Deviation of the mixture's properties from ideal behaviour indicates the specific interactions between components and in this case the increase in ρ , u and n_D implies the presence of attractive forces, assumingly hydrogen bonds, between furfural and furfuryl alcohol. The influence of the composition of the mixture on speed of sound is weaker than on the other studied properties. Furthermore, the addition of small amount of furfural (up to 40%) caused the increase in speed of sound while further increase in furfural fraction led to decrease in speed of sound of binary mixture.

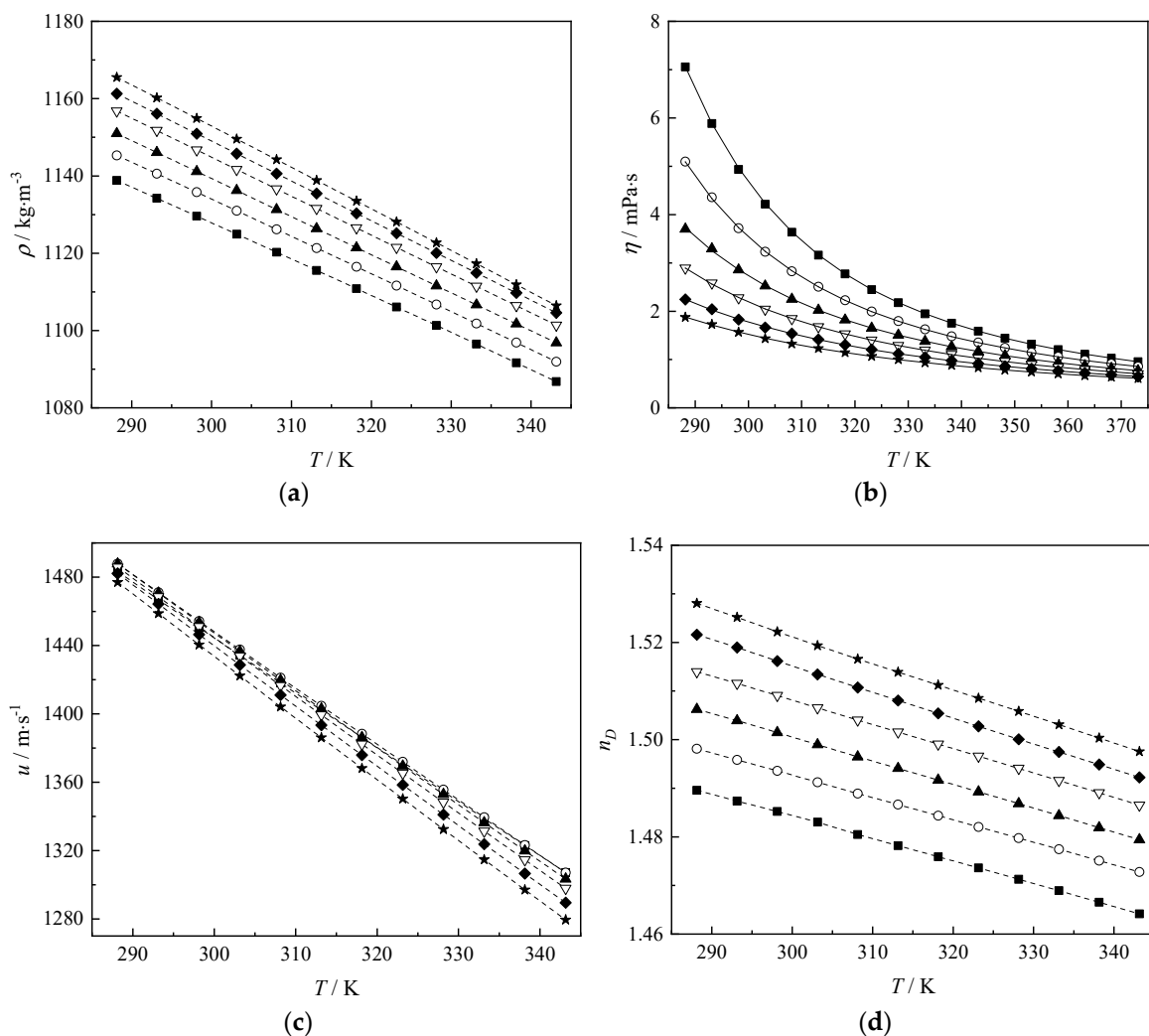


Figure 2. (a) Density, ρ , (b) dynamic viscosity, η , (c) speed of sound, u , and (d) refractive index, n_D , vs. temperature, T , for the binary mixtures furfural (1) + furfuryl alcohol (2) as a function of Furfural mole fraction, x_1 : (■) $x_1 = 0.0000$, (○) $x_1 = 0.2000$, (▲) $x_1 = 0.4000$, (▽) $x_1 = 0.6000$, (◆) $x_1 = 0.8001$, (★) $x_1 = 1.0000$, at 0.1 MPa. Dash lines are guides for the eye, solid lines (b) represent viscosity values calculated using VFT Equation (1).

As for the dependence of viscosity on temperature, it decreases exponentially with temperature elevation, as expected (Figure 2b). The obtained results showed that the increase in the molar fraction of furfural in mixture led to lower viscosity due to lower viscosity of furfural than of furfuryl alcohol. Additionally, the measured viscosities of the studied

mixtures are lower than the values expected for ideal mixture (Grunberg–Nissan rule) indicating the heteromolecular interactions (Figure S1b). Furfural and furfuryl alcohol are both derivatives of furan, where hydrogen at position 2 is substituted with formyl or hydroxymethyl group, respectively (see Table 1). Both compounds have similar densities, higher than water. However, furfuryl alcohol is more viscous comparing to furfural presumably due to hydrogen bonding, especially at lower temperatures. The difference in viscosities diminishes at higher temperatures which might be attributed to the rupture of hydrogen bonding in furfuryl alcohol.

The experimentally obtained viscosity data were fitted to the Vogel–Fulcher–Tammann (VFT) Equation (1) [30–32] leading to the optimized parameters given in Table 3.

$$\ln \eta = A + \frac{B}{T - C} \quad (1)$$

Table 3. Parameters of the Vogel–Fulcher–Tammann equation for furfural (1) + furfuryl alcohol (2) mixtures.

Furfural (1) + Furfuryl Alcohol (2)							
x_1	A	CI _A ^a	B/K	CI _B ^a /K	C/K	CI _V ^a /K	AAD/%
0	−3.34	± 0.04	741.5	± 15	148.1	± 1.8	0.15
0.2000	−3.192	± 0.06	697.6	± 22	143.4	± 2.7	0.16
0.4000	−3.292	± 0.14	752.3	± 55	124.9	± 7.2	0.20
0.6000	−3.113	± 0.12	696.6	± 47	121.3	± 6.8	0.22
0.8001	−3.312	± 0.16	814.9	± 78	90.34	± 11.1	0.19
1	−3.023	± 0.12	698	± 56	97.2	± 9.2	0.17

^a 95% confidence interval.

The obtained good agreement between calculated and measured viscosities (AAD ≈ 0.2%) confirmed the suitability of VFT equation for viscosity correlation (Figure 2b).

Density measurements for pure compounds were also carried out at pressures up to 60 MPa and at temperatures ranging (293.15–413.15) K for furfural and (293.15–373.15) K for furfuryl alcohol (Table 4).

Table 4. Density, ρ , of the pure furfural and furfuryl alcohol at temperatures (293.15–413.15) K and pressures up to 60 MPa.

ρ ^a /kg·m ^{−3}							
Furfural							
T ^b /K							
p ^c /MPa	293.15	303.15	313.15	323.15	333.15	343.15	
0.1	1160.5	1149.8	1139.1	1128.2	1117.3	1106.5	
1	1161.0	1150.4	1139.7	1128.9	1118.0	1107.2	
5	1163.5	1153.0	1142.4	1131.7	1121.0	1110.3	
10	1166.6	1156.2	1145.7	1135.2	1124.7	1114.2	
15	1169.5	1159.3	1149.0	1138.6	1128.2	1117.9	
20	1172.5	1162.4	1152.2	1142.0	1131.8	1121.6	
25	1175.3	1165.4	1155.3	1145.3	1135.2	1125.2	
30	1178.2	1168.3	1158.4	1148.5	1138.5	1128.6	
35	1180.9	1171.2	1161.4	1151.6	1141.8	1132.0	
40	1183.6	1174.0	1164.3	1154.6	1145.0	1135.4	
45	1186.3	1176.8	1167.1	1157.6	1148.1	1138.6	
50	1188.9	1179.5	1170.0	1160.6	1151.1	1141.7	
55	1191.4	1182.1	1172.8	1163.4	1154.0	1144.8	
60	1193.9	1184.7	1175.4	1166.2	1156.9	1147.8	
							T ^b /K

Table 4. Cont.

$\rho^a/\text{kg}\cdot\text{m}^{-3}$						
Furfural						
p^c/MPa	353.15	363.15	373.15	393.15	413.15	
0.1	1095.3	1084.3	1072.6	1050.1	1027.2	
1	1096.1	1085.1	1073.7	1051.2	1028.1	
5	1099.4	1088.6	1077.4	1055.3	1032.7	
10	1103.4	1092.8	1081.8	1060.3	1038.3	
15	1107.4	1097.0	1086.2	1065.1	1043.7	
20	1111.2	1101.0	1090.4	1069.8	1048.8	
25	1115.0	1104.9	1094.6	1074.3	1053.9	
30	1118.6	1108.7	1098.5	1078.7	1058.7	
35	1122.2	1112.4	1102.4	1082.9	1063.3	
40	1125.6	1116.0	1106.2	1087.0	1067.8	
45	1129.0	1119.5	1109.8	1091.0	1072.1	
50	1132.2	1122.9	1113.3	1094.8	1076.2	
55	1135.4	1126.2	1116.7	1098.4	1080.1	
60	1138.5	1129.4	1120.0	1101.9	1083.9	
Furfuryl alcohol						
T^b/K						
p^c/MPa	293.15	303.15	313.15	323.15	333.15	343.15
0.1	1134.6	1125.4	1115.9	1106.5	1097.0	1087.4
1	1135.1	1125.8	1116.5	1107.1	1097.6	1088.0
5	1137.4	1128.0	1118.9	1109.7	1100.2	1090.8
10	1140.2	1130.6	1121.9	1112.8	1103.5	1094.2
15	1142.9	1133.3	1124.8	1115.9	1106.7	1097.4
20	1145.5	1136.0	1127.7	1118.9	1109.8	1100.8
25	1148.2	1138.8	1130.5	1121.8	1112.9	1104.0
30	1150.7	1141.5	1133.3	1124.7	1115.9	1107.1
35	1153.2	1144.2	1136.0	1127.5	1118.8	1110.1
40	1155.7	1147.0	1138.6	1130.2	1121.6	1113.1
45	1158.1	1149.8	1141.2	1132.9	1124.4	1116.0
50	1160.5	1152.6	1143.8	1135.5	1127.1	1118.8
55	1162.8	1155.4	1146.3	1138.1	1129.8	1121.5
60	1165.1	1158.2	1148.7	1140.6	1132.4	1124.2
T^b/K						
p^c/MPa	353.15	363.15	373.15			
0.1	1077.6	1068.0	1058.0			
1	1078.3	1068.7	1059.0			
5	1081.2	1071.8	1062.3			
10	1084.8	1075.5	1066.2			
15	1088.3	1079.2	1070.1			
20	1091.7	1082.8	1073.8			
25	1095.0	1086.2	1077.4			
30	1098.3	1089.6	1081.0			
35	1101.4	1092.9	1084.4			
40	1104.5	1096.1	1087.8			
45	1107.5	1099.2	1091.0			
50	1110.4	1102.2	1094.1			
55	1113.2	1105.2	1097.1			
60	1116.0	1108.0	1100.0			

Expanded uncertainties (95% confidence level, $k = 2$): ^a $U_c(\rho) = 0.9 \text{ kg}\cdot\text{m}^{-3}$ ($293.15 \text{ K} \leq T \leq 363.15 \text{ K}$) and $1.3 \text{ kg}\cdot\text{m}^{-3}$ ($373.15 \text{ K} \leq T \leq 413.15 \text{ K}$); ^b $U(T) = 0.02 \text{ K}$, ^c $U(p) = 0.1 \text{ MPa}$.

Densities of the studied compounds at 0.1 MPa pressure determined using DMA HP device were compared with the values measured by means of DSA 5000 M and the average absolute deviations were 0.01% for furfural and 0.04% for furfuryl alcohol.

Guerrero et al. [22] measured densities of furfural and furfuryl alcohol at temperatures (283.15–338.15) K and pressures up to 60 MPa and their results differ from the data presented in this paper for about 0.02% ($0.3 \text{ kg}\cdot\text{m}^{-3}$) and 0.03% ($0.4 \text{ kg}\cdot\text{m}^{-3}$), respectively. Baird et al. [23] determined the density and vapour pressure of 11 biocompounds in the temperature interval (293.15–423.15) K at pressures up to 10 MPa and one of them was furfural; the agreement between their and the data given here was very good with AAD $\approx 0.03\%$ ($0.4 \text{ kg}\cdot\text{m}^{-3}$).

The experimentally determined densities of the pure compounds as a function of temperature and pressure are presented at Figure 3 showing that the density depends on temperature almost linearly. As expected, an increase in density with pressure rise and decrease in density as a function of increasing temperature was noted for both of the studied compounds.

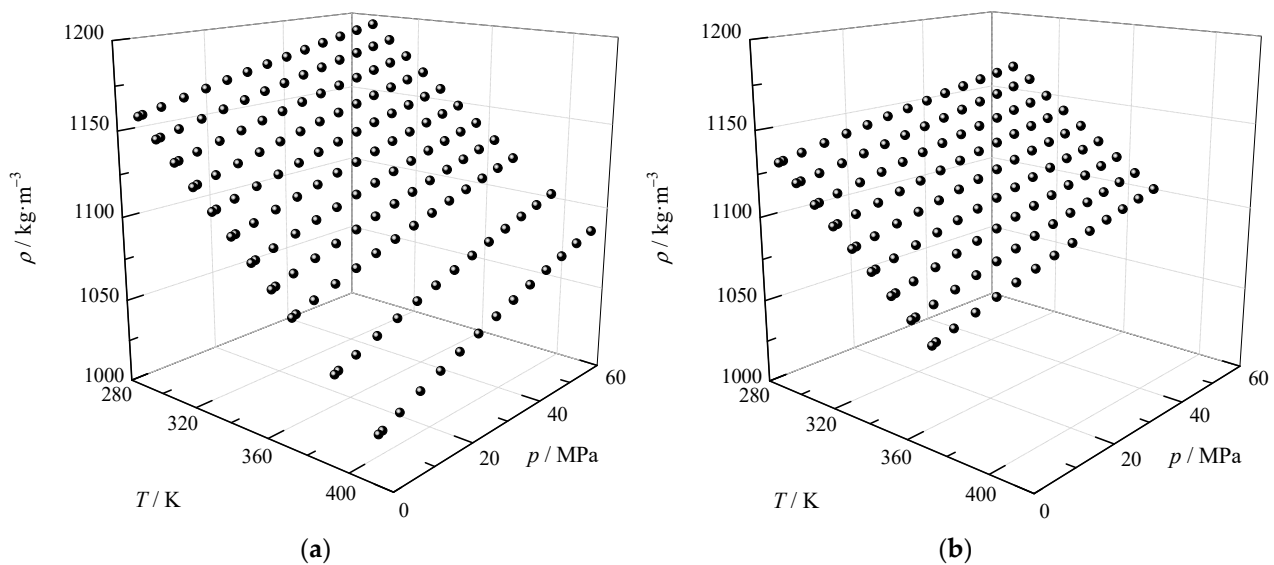


Figure 3. Density, ρ , vs. temperature, T , and pressure, p , for: (a) furfural and (b) furfuryl alcohol.

3.2. High Pressure Density Correlation

The correlation of the experimentally determined high-pressure densities was performed applying the modified Tammann–Tait equation [24] (Equation (2)). That further enabled the calculation of various derived properties.

$$\rho(T, p) = \frac{\rho^{ref}(T, p^{ref})}{1 - C \cdot \ln\left(\frac{B(T)+p}{B(T)+p^{ref}}\right)} \quad (2)$$

where ρ^{ref} represents the density of sample at the reference pressure, $p^{ref} = 0.1 \text{ MPa}$, $B(T)$ is temperature dependent, while C is temperature independent parameter. ρ^{ref} and $B(T)$ are expressed in a form of second-order polynomial:

$$\rho^{ref}(T, p^{ref}) = \sum_{i=0}^2 a_i T^i \quad (3)$$

$$B(T) = \sum_{i=0}^2 b_i T^i \quad (4)$$

where a_i and b_i , in addition to C , are adjustable parameters.

Firstly, for each individual compound, the density data obtained at reference pressure (0.1 MPa) were fitted to Equation (3) which resulted in the determination of parameters

a_i . The parameter optimisation was conducted by applying the Levenberg–Marquardt algorithm [33] aiming to minimize the absolute average deviation between the measured and correlated values. The second step was to adjust parameters b_i and C of Equations (2) and (4) by applying the same optimization procedure to the whole density data set, excluding densities at 0.1 MPa. The optimized parameters of the modified Tammann–Tait equation (Equations (2)–(4)) are given in Table 5. The average absolute percentage deviation (AAD), the maximum percentage deviation (MD), the average percentage deviation (Bias) and the standard deviation (σ) of the experimental data from those calculated using the modified Tammann–Tait equation are also given in Table 5. The low values of AAD (about 0.006%) achieved for both studied pure compounds indicate the good quality of density data modelling.

Table 5. Parameters of the modified Tammann–Tait equation and comparison criteria for furfural and furfuryl alcohol at temperatures (293.15–413.15) K and at pressures up to 60 MPa.

	Furfural	Furfuryl Alcohol
$a_0/\text{kg}\cdot\text{m}^{-3}$	1436.76	1371.86
$a_1/\text{kg}\cdot\text{m}^{-3}\cdot\text{K}^{-1}$	−0.82255	−0.69307
$a_2/\text{kg}\cdot\text{m}^{-3}\cdot\text{K}^{-2}$	−4.0892·10 ^{−4}	−3.9628·10 ^{−4}
b_0/MPa	610.517	489.736
$b_1/\text{MPa}\cdot\text{K}^{-1}$	−1.98354	−1.15038
$b_2/\text{MPa}\cdot\text{K}^{-2}$	1.7018·10 ^{−3}	4.4122·10 ^{−4}
C	0.095393	0.096069
$AAD^a/\%$	0.005	0.009
$MD^b/\%$	0.028	0.10
$Bias^c/\%$	0.005	0.006
$\sigma^d/\text{kg}\cdot\text{m}^{-3}$	0.078	0.199

$${}^a AAD = \frac{100}{N} \sum_{i=1}^N \left| \frac{\rho_i^{\text{exp}} - \rho_i^{\text{cal}}}{\rho_i^{\text{exp}}} \right|; \quad {}^b MD = \max \left(100 \left| \frac{\rho_i^{\text{exp}} - \rho_i^{\text{cal}}}{\rho_i^{\text{exp}}} \right| \right), \quad i = 1, N; \quad {}^c Bias = \frac{100}{N} \sum_{i=1}^N \frac{\rho_i^{\text{exp}} - \rho_i^{\text{cal}}}{\rho_i^{\text{exp}}};$$

$${}^d \sigma = \sqrt{\frac{\sum_{i=1}^N (\rho_i^{\text{exp}} - \rho_i^{\text{cal}})^2}{N-m}}.$$

3.3. Derived Thermodynamic Properties

The knowledge of the density at wide ranges of temperature and pressure enables calculation of various derived volumetric properties. These properties are calculated by differentiating density with respect to pressure or temperature.

The change of density as a response to pressure change is described by the isothermal compressibility, κ_T : [34]

$$\kappa_T = -\frac{1}{V_m} \left(\frac{\partial V_m}{\partial p} \right)_T = \frac{1}{\rho} \left(\frac{\partial \rho}{\partial p} \right)_T = \left(\frac{\partial \ln \rho}{\partial p} \right)_T \quad (5)$$

The incorporation of Equation (2) into (5) gives: [34]

$$\kappa_T = \left(\frac{C}{B(T) + p} \right) \left(\frac{\rho(T, p)}{\rho^{\text{ref}}(T, p^{\text{ref}})} \right) \quad (6)$$

The influence of temperature on density, i.e., the change of density when temperature is changed under constant pressure, is described by the isobaric thermal expansivity, α_p : [34]

$$\alpha_p = -\frac{1}{V_m} \left(\frac{\partial V_m}{\partial T} \right)_p = -\frac{1}{\rho} \left(\frac{\partial \rho}{\partial T} \right)_p = -\left(\frac{\partial \ln \rho}{\partial T} \right)_p \quad (7)$$

The following expression is derived from the modified Tammann–Tait Equations (2) and (7): [34]

$$\alpha_p = - \left[\frac{\rho^{ref'}(T, p^{ref})}{\rho^{ref}(T, p^{ref})} \right] - \frac{C \cdot \frac{B'(T)(p^{ref}-p)}{(B(T)+p)(B(T)+p^{ref})}}{\left(1 - C \cdot \ln \frac{B(T)+p}{B(T)+p^{ref}}\right)} \quad (8)$$

where $\rho^{ref'}(T, p^{ref})$ and $B'(T)$ are derivatives of the parameters $\rho^{ref}(T, p^{ref})$ and $B(T)$ with respect to T , respectively:

$$\rho^{ref'}(T, p) = \sum_{i=0}^2 ib_i T^{i-1} \quad (9)$$

$$B'(T) = \sum_{i=0}^2 ib_i T^{i-1} \quad (10)$$

The thermal pressure coefficient, γ , which represents the ratio between κ_T and α_p , can be calculated as follows: [34]

$$\gamma = \frac{\alpha_p}{\kappa_T} \quad (11)$$

The internal pressure, p_{int} , which gives insight into intermolecular interaction of the sample can be determined using Equation (12): [34]

$$p_{int} = \left(\frac{\partial U}{\partial V} \right)_T = T \left(\frac{\partial P}{\partial T} \right)_\rho - p = T\gamma - p = \frac{T\alpha_p}{\kappa_T} - p \quad (12)$$

where U stands for an internal energy and V is volume of the sample.

Another important thermodynamic property is the difference between the specific heat capacity at constant pressure, c_p , and the specific heat capacity at constant volume, c_v : [34]

$$c_p = c_v + T \frac{(\partial p / \partial T)_\rho^2}{\rho^2 (\partial p / \partial \rho)_T} \quad (13)$$

The coupling of Equations (5) and (7) with (13) leads to the following expression of the mentioned property:

$$c_p - c_v = \frac{\alpha_p^2 T}{\rho \kappa_T} \quad (14)$$

Knowledge on the isothermal and isentropic compressibility enables the calculation of the isobaric specific heat capacity: [35]

$$c_p = \frac{\alpha_p^2 T}{\rho(\kappa_T - \kappa_S)} \quad (15)$$

which is significant for the determination of the isochoric heat capacity using Equation (14).

The calculation of isentropic compressibility, κ_S , requires the knowledge on density and speed of sound: [35]

$$\kappa_S = \frac{1}{\rho u^2} \quad (16)$$

The calculated isothermal compressibility, the isobaric thermal expansivity, the internal pressure and the difference between the isobaric and isochoric specific heat capacities for both examined pure compounds, in the temperature interval (293.15–413.15) K for furfural and (293.15–437.15) K for furfuryl alcohol at pressures up to 60 MPa, are given in the Supplementary Material to the paper (Tables S1 and S2). The isothermal compressibility and the isobaric thermal expansivity calculated for furfural and furfuryl alcohol are presented in Figures 4 and 5.

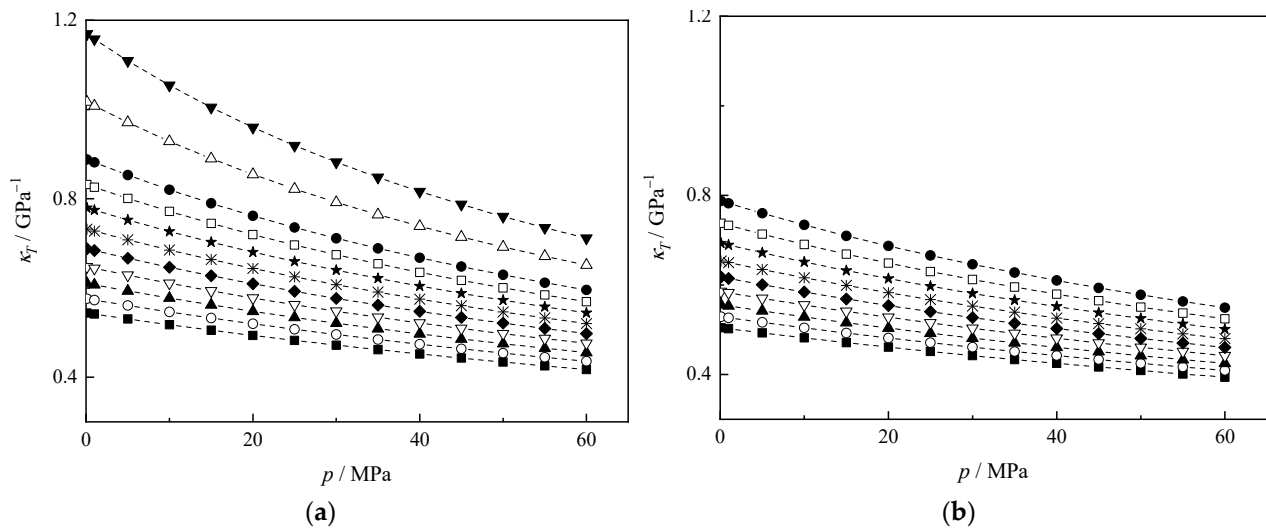


Figure 4. The isothermal compressibility, κ_T , vs. pressure, p , for: (a) furfural and (b) furfuryl alcohol at (■) 293.15 K, (○) 303.15 K, (▲) 313.15 K, (▽) 323.15 K, (◆) 333.15 K, (*) 343.15 K, (★) 353.15 K, (□) 363.15 K, (●) 373.15 K, (△) 393.15 K and (▼) 413.15 K. Dash lines are guides for the eye.

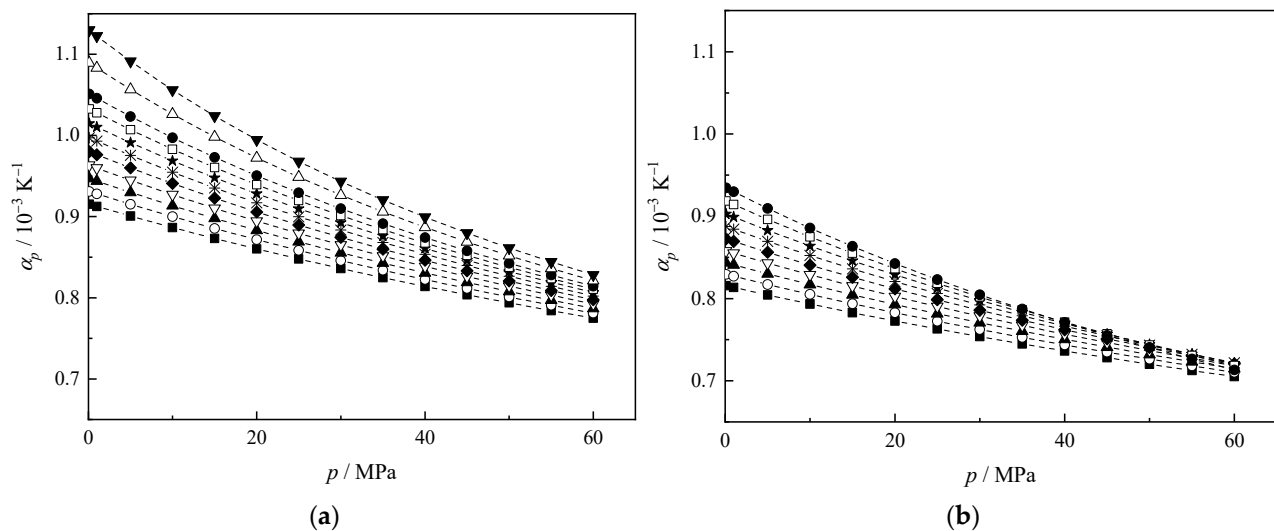


Figure 5. The isobaric thermal expansivity, α_p , vs. pressure, p , for (a) furfural and (b) furfuryl alcohol at (■) 293.15 K, (○) 303.15 K, (▲) 313.15 K, (▽) 323.15 K, (◆) 333.15 K, (*) 343.15 K, (★) 353.15 K, (□) 363.15 K, (●) 373.15 K, (△) 393.15 K and (▼) 413.15 K. Dash lines are guides for the eye.

The isothermal compressibility and the isobaric thermal expansivity of both studied pure compounds increase as temperature rises at constant pressure and decrease with increasing pressure along the isotherms (Figures 4 and 5). The obtained values of κ_T are slightly higher for furfural than for furfuryl alcohol so the change of pressure will affect densities of both compounds similarly. The isothermal compressibility is inversely proportional to the ability of molecules to create hydrogen bonds [22], which could explain the lower values of κ_T obtained for furfuryl alcohol. As for α_p , the calculated values are somewhat higher for furfural than for furfuryl alcohol, meaning that the increase in temperature will cause greater expansion, i.e., a density decrease in the case of furfural than of furfuryl alcohol. This indicates that furfuryl alcohol has a better packed structure than furfural, likely because of stronger intermolecular interactions due to hydrogen bonds that are also known to limit the movement of molecules and that way disable the expansion [12,36]. The isobaric thermal expansivity shows the typical behaviour where its

dependence on temperature becomes weaker with the increase in pressure resulting in the intersection of the isotherms. The intersection point where α_p is temperature independent

$$\left(\frac{\partial \alpha_p}{\partial T}\right)_p = 0$$

was not observed at the studied range of pressure for furfural, while for furfuryl alcohol, it is expected to occur at pressure slightly above 60 MPa.

In addition to this, the isobaric thermal expansivities of both studied compounds were calculated using a pseudo-experimental technique where the measured densities at constant pressure were fitted using polynomial function:

$$\ln(\rho) = a + b \cdot T + c \cdot T^2 \quad (17)$$

The values obtained this way agreed very well with the α_p calculated by differentiating the modified Tammann–Tait equation (Tables S1 and S2); the average absolute percentage deviations for α_p of furfural was less than 0.2% and for furfuryl alcohol it was about 0.5%.

The dependence of the internal pressure on pressure is given in Figure S2. The p_{int} represents the change in internal energy as a result of a very small change in volume at constant temperature and gives insight mainly into weak intermolecular forces such as dispersive, repulsive and dipolar [36]. The internal pressures of the studied compounds are positive implicating the dominant attractive intermolecular forces. The internal pressure decreases with the increase in temperature while pressure does not affect it considerably, especially at lower temperatures, for both studied compounds. The increase in pressure leads to lower values of p_{int} of furfural at temperatures under 343.15 K while at temperatures above 343.15 K p_{int} increases when pressure rises. In the case of furfuryl alcohol, the internal pressure decreases when pressure increases in the whole studied range of temperature indicating that the higher pressure restricts the change of internal energy as a respond to expansion. The p_{int} values calculated for furfural are higher than those obtained for furfuryl alcohol, which is more noticeable at lower temperatures, possibly due to stronger dipole–dipole interactions within more polar furfural when compared with furfuryl alcohol [12]. Although molecules of furfuryl alcohol are linked by hydrogen bonds that are stronger than dipole–dipole interactions between molecules of furfural, hydrogen bonds do not have significant effect on the internal pressure [36].

The isentropic compressibility, κ_S , of furfural and furfuryl alcohol (Table 6) increases with the increase in temperature. A comparison of isothermal (Tables S1 and S2) and isentropic compressibility (Table 6) showed that the values determined for κ_T are for about 25% higher than those calculated for κ_S , for both studied compounds. In general, the ratio κ_T/κ_S is equal to the ratio between isobaric and isochoric heat capacities, C_p/C_V . While isentropic compressibility of furfural at 0.1 MPa is higher than of furfuryl alcohol (for about 6%), the isentropic compressibilities of the examined samples are almost the same. The κ_S of furfuryl alcohol is slightly higher than κ_S of furfural at temperatures up to 313.15 K and at higher temperatures, the relation is reversed.

The calculated values of the specific heat capacities at constant pressure and at constant volume are given in Table 6. The obtained values for both, c_p and c_V , are higher for furfuryl alcohol than furfural. The increase in temperature resulted in the increase in the isobaric and isochoric specific heat capacities and the temperature influence was stronger in the case of furfuryl alcohol.

Table 6. The isentropic compressibility, κ_S , the isobaric specific heat capacity, c_p , and the isochoric specific heat capacity, c_v , of furfural and furfuryl alcohol at 0.1 MPa pressure.

T/K	Furfural			Furfuryl Alcohol		
	κ_S/GPa^{-1}	$c_p/\text{kJ}\cdot\text{kg}^{-1}\cdot\text{K}^{-1}$	$c_v/\text{kJ}\cdot\text{kg}^{-1}\cdot\text{K}^{-1}$	κ_S/GPa^{-1}	$c_p/\text{kJ}\cdot\text{kg}^{-1}\cdot\text{K}^{-1}$	$c_v/\text{kJ}\cdot\text{kg}^{-1}\cdot\text{K}^{-1}$
288.15	0.3933	1.502	1.117	0.3991	1.769	1.433
293.15	0.4050	1.525	1.135	0.4098	1.819	1.479
298.15	0.4173	1.548	1.154	0.4208	1.869	1.523
303.15	0.4300	1.569	1.172	0.4321	1.916	1.565
308.15	0.4433	1.590	1.190	0.4438	1.960	1.605
313.15	0.4570	1.610	1.206	0.4560	2.001	1.642
318.15	0.4713	1.630	1.223	0.4685	2.038	1.675
323.15	0.4862	1.649	1.238	0.4815	2.072	1.705
328.15	0.5017	1.666	1.253	0.4949	2.102	1.731
333.15	0.5178	1.684	1.267	0.5089	2.128	1.753
338.15	0.5346	1.700	1.281	0.5234	2.149	1.771
343.15	0.5521	1.716	1.294	0.5385	2.165	1.785

4. Conclusions

In this work, several thermodynamic and transport properties such as density, viscosity, speed of sound, and refractive index of the binary mixture furfural + furfuryl alcohol were reported at various temperatures and 0.1 MPa. In addition, densities of pure furfural and furfuryl alcohol were determined along with the derived thermodynamic properties at pressures up to 60 MPa over the temperature range from (293.15–413.15) K for furfural and (293.15–373.15) K for furfuryl alcohol.

Experimental results at 0.1 MPa show that furfural has higher density and refractive index than furfuryl alcohol, while viscosities are higher for furfuryl alcohol than furfural. Speeds of sound have more or less similar values, which are more noticeable at low temperatures. All of the studied thermodynamic properties decrease as temperature rises, where the density, speed of sound and refractive index decrease linearly while viscosity depends exponentially on temperature.

Concerning (ρ , p , T) data, as expected, the densities of the examined substances decrease with the increase in temperature and rise when pressure increases. The correlation of the measured high-pressure density data was successfully performed applying the modified Tammann–Tait equation. That further led to the determination of the isothermal compressibility, the isobaric thermal expansivity, the internal pressure and the difference between the isobaric and isochoric specific heat capacities for both examined pure compounds. The isothermal compressibility and the isobaric thermal expansivity are higher for furfural than for furfuryl alcohol and they increase as temperature rises or pressure decreases. The higher values of κ_T and α_p indicate that the change of pressure and temperature will affect density of furfural more than the density of furfuryl alcohol. Furfural also has higher internal pressure in comparison to furfuryl alcohol, which could be the result of the stronger dipole–dipole intermolecular forces within furfural since hydrogen bonds (dominant between molecules of furfuryl alcohol) do not affect the internal pressure.

Supplementary Materials: The following are available online at <https://www.mdpi.com/article/10.3390/en14227769/s1>, Figure S1: (a) Density, ρ , (b) dynamic viscosity, η , (c) speed of sound, u , and (d) refractive index, n_D , vs. furfural mole fraction, x_1 , for the binary mixtures furfural (1) + furfuryl alcohol (2) as a function of temperature, T , at 0.1 MPa, Figure S2: The internal pressure, p_{int} , vs. pressure, p , for: a) furfural and b) furfuryl alcohol at various temperatures, Table S1: The isothermal compressibility, κ_T , the isobaric thermal expansivity, α_p , the difference between isobaric and isochoric specific thermal capacity, $c_p - c_v$, and internal pressure, p_{int} , of furfural, Table S2: The isothermal compressibility, κ_T , the isobaric thermal expansivity, α_p , the difference between isobaric and isochoric specific thermal capacity, $c_p - c_v$, and internal pressure, p_{int} , of furfuryl alcohol.

Author Contributions: Conceptualization, M.L.K. and G.R.I.; methodology, Z.V.S.; investigation, Z.V.S.; resources, M.L.K. and M.G.; data curation, Z.V.S. and G.R.I.; writing—original draft preparation, Z.V.S.; writing—review and editing, I.R.R. and G.R.I.; visualization, I.R.R. and G.R.I.; supervision, I.R.R. and M.L.K.; project administration, M.L.K. and M.G.; funding acquisition, M.L.K. and M.G. All authors have read and agreed to the published version of the manuscript.

Funding: This research was funded by Research Fund of Ministry of Education, Science and Technological of the Republic of Serbia Development (Contract No. 451-03-9/2021-14/200135) and the Slovenian Research Agency (research programme P2-0152 and postdoctoral project Z2-9200).

Institutional Review Board Statement: Not applicable.

Informed Consent Statement: Not applicable.

Data Availability Statement: The data supporting the findings of this study are available within the article and its Supplementary Materials.

Acknowledgments: The authors gratefully acknowledge the Faculty of Technology and Metallurgy, University of Belgrade, Serbia.

Conflicts of Interest: The authors declare no conflict of interest.

References

1. Anastas, P.T.; Warner, J.C. *Green Chemistry: Theory and Practice*; Oxford University Press: New York, NY, USA, 2000.
2. Isikgor, F.H.; Becer, C.R. Lignocellulosic biomass: A sustainable platform for the production of bio-based chemicals and polymers. *Polym. Chem.* **2015**, *6*, 4497–4559. [[CrossRef](#)]
3. Somerville, C.; Youngs, H.; Taylor, C.; Davis, S.C.; Long, S.P. Feedstocks for lignocellulosic fuels. *Science* **2010**, *329*, 790–791. [[CrossRef](#)]
4. Grilc, M.; Likozar, B.; Levec, J. Hydrodeoxygenation and hydrocracking of solvolysed lignocellulosic biomass by oxide, reduced and sulphide form of NiMo, Ni, Mo and Pd catalysts. *Appl. Catal. B Environ.* **2014**, *150–151*, 275–287. [[CrossRef](#)]
5. Mariscal, R.; Maireles-Torres, P.; Ojeda, M.; Sádaba, I.; López Granados, M. Furfural: A renewable and versatile platform molecule for the synthesis of chemicals and fuels. *Energy Environ. Sci.* **2016**, *9*, 1144–1189. [[CrossRef](#)]
6. Mamman, A.S.; Lee, J.M.; Kim, Y.C.; Hwang, I.T.; Park, N.J.; Hwang, Y.K.; Chang, J.S.; Hwang, J.S. Furfural: Hemicellulose/xylose-derived biochemical. *Biofuels Bioprod. Bioref.* **2008**, *2*, 438–454. [[CrossRef](#)]
7. Zhao, Y.; Lu, K.; Xu, H.; Zhu, L.; Wang, S. A critical review of recent advances in the production of furfural and 5-hydroxymethylfurfural from lignocellulosic biomass through homogeneous catalytic hydrothermal conversion. *Renew. Sust. Energ. Rev.* **2021**, *139*, 110706. [[CrossRef](#)]
8. Fele Žilnik, L.; Grilc, V.; Mirt, I.; Cerovečki, Ž. Study of the influence of key process parameters on furfural production. *Acta Chim. Slov.* **2016**, *63*, 298–308.
9. Gómez Millán, G.; Bangalore Ashok, R.P.; Oinas, P.; Llorca, J.; Sixta, H. Furfural production from xylose and birch hydrolysate liquor in a biphasic system and techno-economic analysis. *Biomass Convers. Biorefin.* **2021**, *11*, 2095–2106. [[CrossRef](#)]
10. Lange, J.P. Lignocellulose conversion: An introduction to chemistry, process and economics. In *Catalysis for Renewables: From Feedstock to Energy Production*; Centi, G., van Santen, R.A., Eds.; Wiley-VCH: Weinheim, Germany, 2007; pp. 21–51.
11. Zeitsch, K.J. *The Chemistry and Technology of Furfural and Its Many By-Products*; Elsevier: Amsterdam, The Netherlands, 2000.
12. Lomba, L.; Giner, B.; Bandrés Lafuente, C.; Pino, R. Physicochemical properties of green solvents derived from biomass. *Green Chem.* **2011**, *13*, 2062–2070. [[CrossRef](#)]
13. Bendiaf, L.; Bahadur, I.; Negadi, A.; Naidoo, P.; Ramjugernath, D.; Negadi, L. Effects of alkyl group and temperature on the interactions between furfural and alcohol: Insight from density and sound velocity studies. *Thermochim. Acta* **2015**, *599*, 13–22. [[CrossRef](#)]
14. Zaoui-Djelloul-Daouadji, M.; Bendiaf, L.; Bahadur, I.; Negadi, A.; Ramjugernath, D. Volumetric and acoustic properties of binary systems (furfural or furfuryl alcohol + toluene) and (furfuryl alcohol + ethanol) at different temperatures. *Thermochim. Acta* **2015**, *611*, 47–55. [[CrossRef](#)]
15. De Almeida, B.F.; Waldrigui, T.M.; Alves, T.C.; De Oliveira, L.H.; Aznar, M. Experimental and calculated liquid–liquid equilibrium data for water + furfural + solvents. *Fluid Phase Equilib.* **2012**, *334*, 97–105. [[CrossRef](#)]
16. Hough, E.W.; Mason, D.M.; Sage, B.H. Heat capacities of several organic liquids. *J. Am. Chem. Soc.* **1950**, *72*, 5775–5777. [[CrossRef](#)]
17. Qureshi, M.S.; Vrbka, P.; Dohnal, V. Thermodynamic properties of five biofuel-relevant compounds at infinite dilution in water. *Fuel* **2017**, *191*, 518–527. [[CrossRef](#)]
18. Nduli, M.; Deenadayalu, N. Thermophysical properties of binary mixtures of (methanol or 1-ethyl-3-methylimidazolium acetate + furfural or furfuryl alcohol) at various temperatures. *J. Mol. Liq.* **2017**, *241*, 407–421. [[CrossRef](#)]
19. Mahi, M.R.; Ouaar, F.; Negadi, A.; Bahadur, I.; Negadi, L. Excess/deviation properties of binary mixtures of 2,5-dimethylfuran with furfuryl alcohol, methyl isobutyl ketone, 1-butanol and 2-butanol at temperature range of (293.15–323.15) K. *Oil Gas Sci. Technol. Rev. IFP Energ. Nouv.* **2018**, *73*, 64–78. [[CrossRef](#)]

20. Belhadj, D.; Negadi, A.; Venkatesu, P.; Bahadur, I.; Negadi, L. Density, speed of sound, refractive index and related derived/excess properties of binary mixtures (furfural + dimethyl sulfoxide), (furfural + acetonitrile) and (furfural + sulfolane) at different temperatures. *J. Mol. Liq.* **2021**, *330*, 115436. [[CrossRef](#)]
21. Yan, K.; Wu, G.; Lafleur, T.; Jarvis, C. Production, properties and catalytic hydrogenation of furfural to fuel additives and value-added chemicals. *Renew. Sust. Energ. Rev.* **2014**, *38*, 663–676. [[CrossRef](#)]
22. Guerrero, H.; Lafuente, C.; Rayo, F.; Lomba, L.; Giner, B. $P\rho T$ behavior of several chemicals from biomass. *Energy Fuels* **2011**, *25*, 3009–3013. [[CrossRef](#)]
23. Baird, Z.S.; Uusi-Kyyny, P.; Pokki, J.P.; Pedegert, E.; Alopaeus, V. Vapor pressures, densities, and PC-SAFT parameters for 11 bio-compounds. *Int. J. Thermophys.* **2019**, *40*, 102–137. [[CrossRef](#)]
24. Dymond, J.H.; Malhotra, R. The Tait equation: 100 years on. *Int. J. Thermophys.* **1988**, *9*, 941–951. [[CrossRef](#)]
25. Kijevčanin, M.L.; Živković, E.M.; Djordjević, B.D.; Radović, I.R.; Jovanović, J.; Šerbanović, S.P. Experimental determination and modeling of excess molar volumes, viscosities and refractive indices of the binary systems (pyridine + 1-propanol, +1,2-propanediol, +1,3-propanediol, and +glycerol). New UNIFAC-VISCO parameters determination. *J. Chem. Thermodyn.* **2013**, *56*, 49–56. [[CrossRef](#)]
26. Bajić, D.M.; Živković, E.M.; Jovanović, J.; Šerbanović, S.P.; Kijevčanin, M.L. Experimental measurements and modelling of volumetric properties, refractive index and viscosity of binary systems of ethyl lactate with methyl ethyl ketone, toluene and *n*-methyl-2-pyrrolidone at 288.15–323.15 K and atmospheric pressure. New UNIFAC-VISCO and ASOG-VISCO interaction parameters. *Fluid Phase Equilib.* **2015**, *399*, 50–65.
27. Chirico, R.D.; Frenkel, M.; Magee, J.W.; Diky, V.; Muzny, C.D.; Kazakov, A.F.; Kroenlein, K.; Abdulagatov, I.; Hardin, G.R.; Acree, W.E.J.; et al. Improvement of quality in publication of experimental thermophysical property data: Challenges, assessment tools, global implementation, and online support. *J. Chem. Eng. Data* **2013**, *58*, 2699–2716. [[CrossRef](#)]
28. Comuñas, M.J.P.; Bazile, J.P.; Baylaucq, A.; Boned, C. Density of diethyl adipate using a new vibrating tube densimeter from (293.15 to 403.15) K and up to 140 MPa. Calibration and measurements. *J. Chem. Eng. Data* **2008**, *53*, 986–994. [[CrossRef](#)]
29. Ivaniš, G.R.; Tasić, A.Ž.; Radović, I.R.; Đorđević, B.D.; Šerbanović, S.P.; Kijevčanin, M.L. An apparatus proposed for density measurements in compressed liquid regions at the pressures 0.1–60 MPa and the temperatures 288.15–413.15 K. *J. Serb. Chem. Soc.* **2015**, *80*, 1073–1085. [[CrossRef](#)]
30. Vogel, H. The temperature dependence law of the viscosity of fluids. *Phys. Z.* **1921**, *22*, 645.
31. Fulcher, G.S. Analysis of recent measurements of the viscosity of glasses. *J. Am. Ceram. Soc.* **1925**, *8*, 339. [[CrossRef](#)]
32. Tammann, G.; Hesse, W. Die Abhängigkeit der Viscosität von der Temperatur bei unterkühlten Flüssigkeiten. *Z. Anorg. Allg. Chem.* **1926**, *156*, 245. [[CrossRef](#)]
33. Marquardt, D.W. An algorithm for least-squares estimation of nonlinear parameters. *J. Appl. Math.* **1963**, *11*, 431–441. [[CrossRef](#)]
34. Ivaniš, G.R.; Tasić, A.Ž.; Radović, I.R.; Đorđević, B.D.; Šerbanović, S.P.; Kijevčanin, M.L. Modeling of density and calculations of derived volumetric properties for *n*-hexane, toluene and dichloromethane at pressures 0.1–60 MPa and temperatures 288.15–413.15 K. *J. Serb. Chem. Soc.* **2015**, *80*, 1423–1433. [[CrossRef](#)]
35. Aissa, M.A.; Ivaniš, G.R.; Radović, I.R.; Kijevčanin, M.L. Experimental investigation and modeling of thermophysical properties of pure methyl and ethyl esters at high pressures. *Energy Fuels* **2017**, *31*, 7110–7122. [[CrossRef](#)]
36. Aparicio, S.; Alcalde, R. The green solvent ethyl lactate: An experimental and theoretical characterization. *Green Chem.* **2009**, *11*, 65–78. [[CrossRef](#)]